General and Comparative Endocrinology 274 (2019) 60–72

Contents lists available at ScienceDirect

General and Comparative Endocrinology

journal homepage: www.elsevier.com/locate/ygcen

Comparative transcriptomic characterization of the eyestalk in Pacific white shrimp (*Litopenaeus vannamei*) during ovarian maturation

Zhongkai Wang[a,b], Sheng Luan[a,b], Xianhong Meng[a,b], Baoxiang Cao[a,b], Kun Luo[a,b], Jie Kong[a,b,*]

[a] Key Laboratory for Sustainable Utilization of Marine Fisheries Resources, Ministry of Agriculture, Yellow Sea Fisheries Research Institute, Chinese Academy of Fishery Sciences, Qingdao 266071, China

[b] Laboratory for Marine Fisheries Science and Food Production Processes, Qingdao National Laboratory for Marine Science and Technology, Qingdao 266071, China

ARTICLE INFO

Keywords:
Litopenaeus vannamei
Reproduction
Eyestalk
Transcriptome
Exoskeleton formation

ABSTRACT

In crustaceans, some of fundamental regulatory processes related to a range of physiological functions, including ovarian maturation, molting, glucose homeostasis, osmoregulation, etc., occur in the organs of the eyestalk. Additionally, reproduction is regulated by neuropeptide hormones and other proteins released from secretory sites (X-organ/sinus gland, XO/SG) within the eyestalk. As unilateral eyestalk ablation was the most common method used to artificially induce ovarian maturation for farmed *Litopenaeus vannamei*, to better understand the reproductive regulation mechanism in *L. vannamei*, we have investigated the transcriptomes of the eyestalk during five ovary developmental stages with or without eyestalk ablation by high-throughput Illumina sequencing technology. The raw reads were assembled and clustered into 127,031 unigenes. Meanwhile, the differentially expressed genes (DEGs) between ovarian development stages were identified. We examined, through DEG enrichment analysis, eyestalk gene expression patterns for Gene Ontology (GO) and Kyoto Encyclopedia of Genes and Genomes (KEGG) pathways, comparing natural to artificially induced ovarian maturation. We also identified a variety of transcripts that appear to be differentially expressed throughout ovarian maturation. These include transcripts that encode G-protein coupled receptors (GPCRs) and neuropeptides, such as the crustacean hyperglycemic hormone (CHH), molt-inhibiting hormone (MIH), and crustacean female sex hormone (CFSH). Furthermore, numerous exoskeleton formation-related genes were found to be down-regulated during ovarian maturation, including cuticle-like proteins, eclosion hormone (EH), and gastrolith-like proteins, of which the latter are the first reported in *L. vannamei*. Our work is the first reproduction-related investigation of *L. vannamei* focusing on the eyestalk at the whole transcriptome level. These findings provide novel insight into the function of the eyestalk in reproduction regulation.

1. Introduction

The Pacific white shrimp, *Litopenaeus vannamei*, is one of the most important farmed penaeid shrimp species in the world. The most common method used to stimulate ovarian maturation and spawning during captive breeding of *L. vannamei* is unilateral eyestalk ablation. While ablation can induce ovarian maturation, it also jeopardizes growth, increases energetic demands, and causes a significant hormonal imbalance that has a considerable impact on the quantity, quality, and survival of the larvae produced (Benzie, 1998; Browdy and Samocha, 1985; Palacios et al., 1999). Thus, predictable maturation and spawning in farmed shrimp without eyestalk ablation is a long-term goal for the shrimp culture industry.

A better understanding of the hormonal regulation of shrimp reproduction would allow for the development of methods for manipulation of reproduction without eyestalk ablation. Endocrine control of crustacean reproduction is an area that has received considerable attention, with emphasis placed on the roles of the eyestalk neuropeptides and hormones. The crustacean eyestalk is where the X-organ/sinus gland (XO/SG) complex is located, and is an important neuroendocrine system (Christie et al., 2010b; Webster et al., 2012). The XO/SG complex is the main site of production and storage of the crustacean hyperglycemic hormone (CHH) superfamily, which includes the CHH, the molt-inhibiting hormone (MIH), the gonad-inhibiting hormone (GIH), and the mandibular organ-inhibiting hormone (MOIH), and the chromatophorotropins, including the pigment dispersing hormone (PDH)

* Corresponding author at: Key Laboratory for Sustainable Utilization of Marine Fisheries Resources, Ministry of Agriculture, Yellow Sea Fisheries Research Institute, Chinese Academy of Fishery Sciences, Qingdao 266071, China (J. Kong).

E-mail addresses: zkwang@mail.ustc.edu.cn (Z. Wang), luansheng@ysfri.ac.cn (S. Luan), mengxianhong@ysfri.ac.cn (X. Meng), luokun@ysfri.ac.cn (K. Luo), kongjie@ysfri.ac.cn (J. Kong).

https://doi.org/10.1016/j.ygcen.2019.01.002
Received 1 February 2018; Received in revised form 2 January 2019; Accepted 2 January 2019
Available online 03 January 2019

and the red pigment concentrating hormone (RPCH). These neuropeptides control many fundamental physiological functions such as molting, osmoregulation, modulation of glycemia, and reproduction (Christie et al., 2010b; Hopkins, 2012; Manfrin et al., 2015).

Because the effect of eyestalk ablation has been attributed to a reduction in the normal levels of GIH in the neurosecretory cells of the eyestalk (Hopkins, 2012), the GIH, also known as vitellogenesis-inhibiting hormone (VIH), is the most potent known inhibitor of gonadal maturation. Thus, in previous studies, molecular research on the reproductive regulation of eyestalk in *L. vannamei* has mostly concentrated on identifying and cloning such regulatory genes. Several neuropeptide genes related to reproductive regulation were PCR amplified and sequenced. Seven peptides (designated as SGP-A, -B, -C, -D, -E, -F, and -G) of the CHH family were purified by reversed-phase HPLC, identified by N-terminal amino acid sequencing from the sinus glands of *L. vannamei*, and examined for their regulatory effects on vitellogenin (*Vg*) mRNA expression using *in vitro* incubation of ovarian fragments (Tsutsui et al., 2007). Furthermore, the cDNA sequence of *L. vannamei* SGP-G (Liv-SGP-G) was cloned, and the vitellogenesis inhibiting activity of recombinant Liv-SGP-G was examined *in vitro* using ovarian fragments (Tsutsui et al., 2013). Another candidate gene, *LvVIH*, was characterized and its reproduction inhibitory effect was confirmed by both *in vitro* and *in vivo* approaches (Chen et al., 2014). In addition, MIH is another potential reproductive regulator. In *L. vannamei*, two forms of MIH-like genes (*LivMIH1* and *LivMIH2*) were cloned and characterized, and the LivMIH2 protein positively regulated hepatopancreatic *Vg* gene expression (Chen et al., 2007; Luo et al., 2015). However, the information collected using these methods was incomplete and provided only a fragmented picture. The molecular mechanisms by which the eyestalk regulates ovarian development remain unclear. The next-generation RNA-sequencing method, which can be used to compare a few genes to the entire transcriptome, could be a vital approach in understanding this ontology. This technology has dramatically improved the efficiency and speed of analysis, especially for non-model species, which has been widely applied to studies in *L. vannamei* (Dai et al., 2017; Gao et al., 2017; Lu et al., 2016; Wei et al., 2014). Therefore, it is considered to be a powerful tool for dissecting gene networks associated with particular biological and developmental processes at the whole transcriptome level.

To investigate and gain a better understanding of the regulation mechanism of the eyestalk in *L. vannamei*, we analyzed the transcriptomic characterization of the eyestalk during five dynamic ovarian developmental stages through Illumina high-throughput sequencing data. To our knowledge, this is the first transcriptome wide gene expression profiling of the eyestalk in *L. vannamei*. This study will be a foundational resource for further studies in reproductive regulation mechanisms.

2. Materials and methods

2.1. Animal origin and acclimatization

One hundred adult females (34–45 g body weight) were stocked in the shrimp reproduction laboratory at Hebei Xinhai Aquatic Biotechnology Co., Ltd. These females were stocked equally in two ponds at a density of 5 shrimp per square meter. The water was exchanged daily (95%). The temperature was maintained at 28 °C. The salinity was maintained at 30 ppt.

2.2. Experiment design

Before the experiment, the shrimp were fed commercial diets. Then, they were fed fresh bait when the experiment began. The diet was composed of 40% squid and 60% rag worm. It was divided into four equal daily rations that accounted for a total daily supply of 20% of wet weight biomass and was adjusted daily. Ovarian development was assessed daily by observing the size and color of gonads with a lamp. Macroscopically, developmental stages of the ovary were classified by the appearance of the ovary at the cephalothorax region or along the abdominal back that could be seen through the dorsal exoskeleton. The criteria for ovary staging were as follows: S0 stage (immature), undeveloped ovaries were not visible in either the cephalothorax region or along the abdominal back; S1 stage (early maturation), there were enlarged ovaries in the cephalothorax region, and they could be observed as a thin line through the dorsal exoskeleton; S2 stage (intermediate maturation), the ovaries appeared as a yellowish linear band through the dorsal exoskeleton; S3-4 stage (mature), the ovaries started to become orange-colored, appearing as a double thick line along the abdominal back with larger expansion at the posterior thorax (adapted from (Tan-Fermin and Pudadera, 1989)). The molting cycle of the shrimp was also recorded. According to the appearance of the epidermis, pigmentation, the formation of new setae, and the presence of matrix or internal cones in the setal lumen (Corteel et al., 2012; Jrdeo et al., 2006), the molt stage of the shrimp was determined through the morphological observation of uropod under a light microscope.

The eyestalks of the shrimp used in this study were not ablated at the beginning of the experiment. They were cultivated with the eyestalk intact for natural maturation during the following 50 days. At the end of the 50-day cultivation, there were five shrimp with ovaries at S3-4 stage, two shrimp at S1 stage, and one shrimp at S2 stage, and others were still at S0 stage. Then, the five shrimp with ovaries at S3-4 stage were dissected, and the eyestalks (E4) were separately flash frozen in liquid nitrogen and then kept at −80 °C until RNA isolation. Five shrimp with ovaries still at S0 stage were also dissected, and the eyestalks (E0) were separately collected as described above. After that, other shrimp at S0 stage were subjected to unilateral eyestalk ablation to artificially induce ovarian maturation. These shrimp were also stocked equally in two ponds. During the following week, the eyestalks (E1, E2, E3) of five S1, S2, and S3-4 females were separately collected as well. The ovaries of 5 shrimp for each ovarian development stage were dissected and weighed, and a portion of the lateral lobe was flash frozen in liquid nitrogen for RNA isolation or fixed in Bouin's solution for histological analysis (Fig. S1). In addition, the shrimp were weighed to calculate the gonadsomatic index (GSI) to further assess the development of the ovaries (Table S1). Besides, all the shrimp were sampled in the inter-molt stage.

2.3. RNA isolation and quality control

Total RNA was separately isolated from the each eyestalk or ovary using TriPure isolation reagent kit (Roche Diagnostics, USA) according to the manufacturer's instruction. The genomic DNA was cleaned from RNA with RNase free DNase I (Takara, China), and the degradation and contamination of RNA was monitored by running samples on 1.5% agarose gels. The RNA purity was checked using a NanoPhotometer spectrophotometer (Implen, Germany). The RNA concentration was measured using a Qubit RNA Assay Kit in Qubit 2.0 Fluorometer (Life Technologies, USA). The RNA integrity was assessed using the RNA Nano 6000 Assay Kit for the Bioanalyzer 2100 system (Agilent Technologies, USA) and expressed as an RNA Integrity Number (RIN). According to the results, all of the RNA samples were high quality (OD260/280 = 2.0–2.2, OD260/230 ≥ 2.0, RIN ≥ 8.0, and 28S:18S ≥ 1.0).

2.4. Library construction and Illumina sequencing

RNA samples of the five eyestalks from the same ovarian developmental stages were pooled together in equal amounts to generate one mixed sample. A total amount of 3 μg of high-quality RNA was used for library construction. These five RNA samples (E0-E4) were used to construct individual cDNA libraries (Lu et al., 2016). The cDNA libraries were sequenced on an Illumina HiSeq2500 platform at

Annoroad Genomics (Beijing, China) and 150 bp pair-end reads were generated.

2.5. De novo transcriptome assembly and functional annotation

The adapter-polluted sequences, low-quality reads, and reads with unknown nucleotides larger than 5% were removed from the raw reads by Cutadapt (Martin, 2011) and Fqtools developed by ANOROAD. Then, the high-quality reads were used for downstream analysis. The clean reads were then assembled using Trinity software (v.20140717) to obtain transcripts with an optimized k-mer length of 25 and all other parameters were set to default (Grabherr et al., 2011). The longest assembled non-redundant transcripts were referred to as unigenes.

The assembled transcripts were translated into all six possible open reading frames (ORFs) through TransDecoder (v.20140717), and their proper translation was defined as the one that gave the longest amino acid sequence (Saha et al., 2002). Then, Trinotate (v.20140717) was used for performing the functional annotation of unigenes. All unigenes and ORFs were used as queries to align against sequences in NCBI non-redundant nucleotide/protein database (NT and NR databases), Universal Protein Resource (UniProt) database, Gene Ontology (GO), Cluster of Orthologous Groups of proteins (COG), and Kyoto Encyclopedia of Genes and Genomes (KEGG) database with an E-value cut-off of 1.0e-5. The NR/NT and UniProt databases were downloaded on October 9, 2016.

2.6. Analysis of differentially expressed unigenes

Reads counts for each gene in each sample were counted by HTSeq v0.6.0, and the RPKM (reads per kilobase million mapped reads) was then calculated to estimate the expression level of genes in each sample (Mortazavi et al., 2008). The RPKM eliminated the effect of sequencing depth and gene length on gene expression levels, enabling direct comparison among the data. DEGseq v1.18.0 was used for differential gene expression analysis between samples (E0-E1, E1-E2, E2-E3, E3-E4, and E4-E0) (Wang et al., 2010). The *p*-value was assigned to each gene and adjusted by the Benjamini and Hochberg's approach as *q*-value for controlling the false discovery rate (FDR). Genes with $q < 0.05$ and $|\log_2\text{Ratio}| \geq 1$ are identified as differentially expressed genes (DEGs).

The GO enrichment analysis of DEGs was implemented by the GOseq R package, and enrichment analysis was also performed to identify the DEGs that were significantly enriched in KEGG pathways with the KOBAS software (Wu et al., 2006). The GO terms and KEGG pathways enrichment of DEGs were implemented by a hypergeometric test, in which the *p*-value was calculated and adjusted as a *q*-value, and the data background were genes of the whole transcriptome. GO terms or KEGG pathways with $q < 0.05$ were considered to be significantly enriched.

2.7. Validation by real-time quantitative PCR

To verify the accuracy of RNA-seq data, twelve unigenes were selected for verification by qPCR amplification with gene-specific primers designed by Primer 5.0 (Table S2). The RNA samples used here were separately isolated from the eyestalk or ovary from the same animals used for RNA-seq analysis as described above. Amplification reactions were examined by gel electrophoresis to confirm a single product of the expected size and the efficiency of the primers was examined by Real-time PCR Miner (Zhao and Fernald, 2005). Then, these specific PCR products were verified through sequencing.

qPCR was performed in a 20 μl solution containing 20 ng template cDNA and THUNDERBIRD SYBR qPCR Mix (TOYOBO, Japan) via the ABI7500 system (Applied Biosystems, USA) at 98 °C (5 min) for pre-incubation, followed by 40 cycles at 98 °C (10 s), 60 °C (10 s) and 68 °C (40 s). Finally, the melting curve was analyzed to detect single amplification. The accumulation of fluorescent signal from SYBR Green was recorded at the 68 °C (40 s) phase during each cycle. A negative control (no-template reaction) was always included. Three biological replicates of each sample were analyzed, with each sample run in triplicate.

β-actin and EF1α were used as reference genes, and the relative expression level was normalized by geometric averaging of the two host genes (Vandesompele et al., 2002). The relative gene expression levels were calculated using the comparative Ct method with the formula $2^{-\triangle\triangle Ct}$ (Livak and Schmittgen, 2001). The relative expression level of β-actin or EF1α was calculated with the other gene as a reference gene. qPCR data were statistically analyzed by one-way ANOVA followed by a Tukey's post hoc test using SPSS 20.0 (SPSS, IL, USA), and $p < 0.05$ denotes a statistically significant difference. The qPCR results were then compared with transcriptome data (RPKM value) to detect their expression correlation of each gene.

3. Results

3.1. Transcriptome sequencing and assembly

Five cDNA libraries were constructed on the basis of 25 RNA samples as described. The overall Illumina sequencing data were deposited in the Short Read Archive database of NCBI (SRR6488339, SRR648838, SRR6488341, SRR6488340, and SRR6488337), which contained 268,684,708 raw reads (Table S3). After removing adaptors and trimming low quality reads, 235,094,096 clean reads were obtained.

The clean bases were used to perform *de novo* assembly and were assembled into 150,127 transcripts with a total length of 108,551,181 nucleotides (Table 1). The average percentage of GC content for the transcripts was 43.07%. The length of the transcripts ranged from 201 bp to 79,844 bp with an average length of 723 bp. The lengths of N50 and N90 of the transcripts were 1,363 bp and 263 bp, respectively. These transcripts were subsequently assembled into 127,031 unigenes with an average length of 625 bp. The lengths of N50 and N90 of the unigenes were 1,024 bp and 249 bp, respectively. The data was deposited in the Transcriptome Shotgun Assembly database of NCBI (accession number: GGQV00000000). The total length of the unigenes was 79,372,773 bp, which covered 73.12% of the length of transcripts. The assembly efficiency was further validated by Bowtie2 (v2.2.3) (Langmead and Salzberg, 2012), and the percentage of individual library reads that mapped back to the assembled transcriptome was 83.98%, 87.38%, 89.06%, 87.99%, and 89.25%, respectively.

3.2. Functional annotation of unigenes

In our analysis, 27,583 unigenes that were predicted to have ORFs were acquired, which represent 21.71% of the total assembled unigenes. The lengths of the predicted ORFs range from 297 to 13,233 bp, with an average length of 949 bp. The assembled unigenes and predicted ORFs were subjected to similarity analysis in public databases. The maximum number of 28,879 unigenes matched the NR database, followed by UniProt (23,637 unigenes) and NT (4326 unigenes). A total of 13,910 ORFs were annotated in the UniProt database. The Venn diagram (Fig. S2) illustrates the interrelation of Blast hits for unigenes

Table 1
Summary of de novo assembly results of the transcriptome.

Basic Stat	Trinity	Unigene
N50	1363	1024
N90	263	249
Min length	201	201
Max length	79,884	79,884
Mean length	723	625
Count	150,127	127,031
Percent GC (%)	43.07	42.51
Total Bases	108,551,181	79,372,773

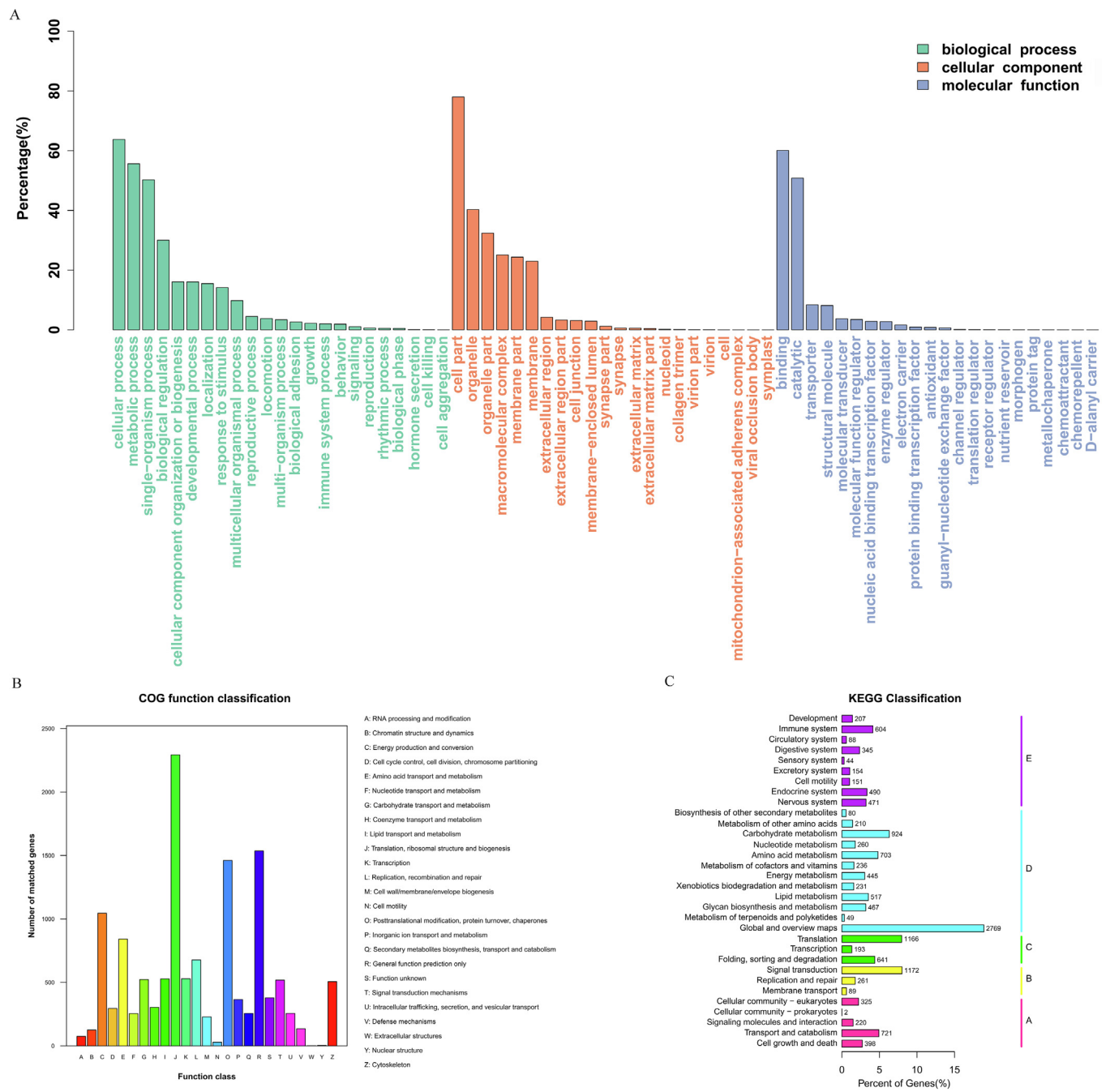

Fig. 1. Gene ontology (GO), Clusters of Orthologous Group (COG), and Kyoto Encyclopedia of Genes and Genomes (KEGG) classification of all unigenes. (A) The GO classification results summarized in three main GO categories (cellular component, molecular function, and biological process). The x-axis represents the GO ontology. The y-axis indicates the percentage of unigenes. (B) COG classification of all unigenes. The columns with different colors represent the number of unigenes in different subcategory. (C) KEGG classification of all unigenes. The columns represent the number of unigenes in each subcategory.

and ORFs against three databases.

A total of 23,218 unigenes were successfully annotated by Gene Ontology (GO) assignments and were classified into three functional categories, namely, biological process, molecular function, and cellular component (Fig. 1A). The biological process category was grouped to 23 subcategories, among which the major subcategories were cellular process (63.77%) and metabolic process (55.62%). The cellular component category contained 22 subcategories, among which cell part (77.98%) and organelle (40.28%) were the dominant subcategories. In the molecular function category, the major subcategories were binding (60.07%) and catalytic (50.83%).

As for Clusters of Orthologous Groups (COG), 11,474 unigenes were classified into 25 functional categories (Fig. 1B). The dominant categories included (J) Translation, ribosomal structure and biogenesis, (R) General function prediction only, (O) Posttranslational modification, protein turnover, chaperones, (C) Energy production and conversion, and (E) Amino acid transport and metabolism.

The biological pathways for the unigenes were searched using the Kyoto Encyclopedia of Genes and Genomes (KEGG) database, by which 14,633 unigenes were assigned to 5 special KEGG pathways, including Metabolism (D, 47.08%), Organismal Systems (E, 17.45%), Genetic Information Processing (C, 13.67%), Cellular Processes (A, 11.38%), and Environmental Information Processing (B, 10.40%) (Fig. 1C). The annotated unigenes were involved in 324 different pathways. Among

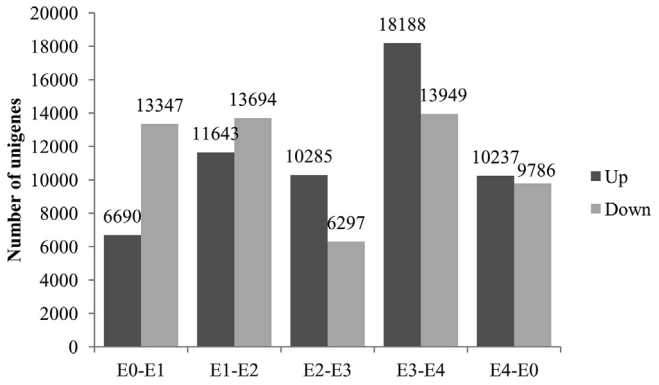

Fig. 2. Statistics of differentially expressed genes between samples. Black columns represent the number of up-regulated genes while gray columns represent the number of down-regulated genes.

all the KEGG classifications, the largest number of unigenes (2769) were assigned to the 'Global and overview maps' pathway, accounting for 40.18% of the total annotated unigenes in the category of Metabolism, followed by the 'Signal transduction' pathway (1172 unigenes) and the 'Translation' pathway (1166 unigenes) in the categories of Environmental Information Processing and Genetic Information Processing, respectively. Additionally, there were 471 and 490 unigenes separately identified in the 'Nervous system' and 'Endocrine system' pathways in the category of Organismal Systems.

3.3. DEGs between different phases of ovarian development

To identify DEGs involved in ovarian development, we used the RPKM value to compare the expression differences between different groups. A large number of DEGs were screened with adjusted $q < 0.05$ and $|\log_2\text{Ratio}| \geq 1$ (Fig. 2; Fig. S3). Of all the Trinity assemblies (127,031 unigenes), 20,037 unigenes were identified as DEGs between E0 and E1 (6690 up-regulated and 13,347 down-regulated in the E0 samples), and 25,337 were identified as DEGs between E1 and E2 (11,643 up-regulated and 13,694 down-regulated in E1). The number of DEGs distinctly decreased when comparing E2 with E3 (16,582 DEGs with 10,285 up-regulated, 6,297 down-regulated in E2), and increased to the largest when comparing E3 with E4 (32,137 DEGs with 18,188 up-regulated and 13,949 down-regulated in E3). The number of up-regulated DEGs was slightly more than that of down-regulated DEGs when comparing E4 with E0 (20,023 DEGs with 10,237 up-regulated and 9,786 down-regulated in E4).

3.4. Functional enrichment analysis of GO terms and KEGG pathways

GO term and KEGG pathway enrichment analyses were able to improve our understanding of the underlying biological processes related to various biological traits. GO term enrichment analysis detected significantly overrepresented GO terms in DEGs with adjusted $q < 0.05$. The top five most significantly enriched GO terms are shown in Table 2, including the q-value of the GO term and the number of up- and down-regulated genes enriched in each GO term. The biological process terms described a series of events accomplished by one or more organized assemblies of molecular functions. For the five comparison groups, 'translation' was the process with the highest enrichment level except in the E3-E4 group. Other significant biological process terms include 'protein metabolic process' and 'small molecule metabolic process'. The molecular function terms provided insight into the elemental activities that occur at the molecular level. For E0-E1, E1-E2, E2-E3, and E4-E0 groups, 'structural molecule activity', 'structural constituent of ribosome', and 'structural constituent of cuticle' were all listed in the top five molecular function terms. In addition, the 'ribosome', 'ribonucleoprotein complex', 'cytosolic ribosome', and 'extracellular region' were listed together in the top five cellular component terms in E0-E1, E2-E3, and E4-E0 groups.

To evaluate the pathways associated with DEGs, we conducted the KEGG pathway enrichment analysis. The top five enriched pathways are listed in Table 3, including the number of up-regulated and down-regulated genes enriched in each pathway. The 'ribosome' pathway, with the highest enrichment level and the highest number of DEGs, was enriched in E0-E1, E1-E2, E2-E3, and E4-E0 groups, and it was also listed with the highest number of DEGs among the top five enriched pathways in E3-E4 group.

3.5. Identification of functional unigenes during ovarian development

In this study, nineteen unigenes encoding putative neuropeptides were identified by Blast searching of all the transcripts against the public database (Table 4). Among them, four unigenes were annotated as CHH superfamily members. Moreover, the expression of two unigenes (c108833_g1, c103865_g1) was significantly increased in the E1 and E3 stages after the eyestalk was ablated. We also performed qPCR analysis to further confirm their expression patterns (Fig. 3A). The peptide encoded by unigene (c108833_g1) showed very high similarities with the genes LvITP (GenBank: ABN11282.1) and CHH-B1 (GenBank: AAN86056.1) from *L. vannamei* (Fig. S4A). The peptide encoded by the other unigene (c103865_g1) was identified with the molting-inhibiting hormone-like (MIHL) protein from *L. vannamei* (GenBank: ATN45407.1) (Fig. S4B). In addition, sequence alignment showed that the unigene (c24357_g1) had a high similarity with the neuropeptide SGP-G of *L. vannamei* (GenBank: AB744717) (Fig. S4C), but its expression was hardly detected. Another unigene (c122023_g1) showed considerable expression levels with no significant changes during ovarian development and was identified with the CHH gene from *L. vannamei* (GenBank: KJ660842.2).

Except for the CHH superfamily, the expression of the unigene (c15356_g1) annotated as the crustacean female sex hormone (CFSH) was significantly increased at the E4 stage (Fig. 3A). We further examined the expression profiles of this putative Liv-CFSH gene and vitellogenin (Liv-Vg) gene in the ovary during ovarian maturation. We could only detect the expression of Liv-Vg in the ovary with high expression levels at the S2 stage (Fig. S5), while there was no expression of the unigene (c15356_g1) in the ovary during ovarian maturation.

In addition to the neuropeptides, we also screened fourteen G-protein coupled receptors (GPCRs), which showed lower expression levels in the E0 and E4 stages when the eyestalks were not ablated, while they showed higher expression levels in the E1, E2, and E3 stages after unilateral eyestalk ablation (Fig. 4).

We also screened and characterized a series of unigenes that showed similar expression patterns during ovarian maturation. A total of 104 unigenes were identified to be significantly down-regulated (Table S4), and 29 unigenes were significantly up-regulated (Table S5) from the E0 stage to the E3 stage when screened with adjusted $q < 0.05$ and $|\log_2\text{Ratio}| \geq 1$. For the up-regulated genes, only seven genes have been annotated, and none of the genes have homology to known proteins of aquatic species related to ovarian maturation. For the down-regulated genes, 25 genes were shown to function in exoskeleton formation, including one gene (c106238_g1) annotated as eclosion hormone (EH) and other genes annotated as cuticle protein or calcification-associated protein (Fig. 5). Multiple sequence alignment revealed that the predicted EH-like peptide of *L. vannamei* showed a high similarity with those from other species and all EH sequences shared six conserved cysteine residues in the eclosion domain (Fig. S6). Phylogenetic analysis showed that this EH was most closely related to EH from another crustacean species, *Callinectes sapidus*, then to EHs from other crustacean species, and finally to EHs from insects (Fig. S7). The expression levels of those exoskeleton formation-related genes were highest at the E0 stage and drastically decreased with ovarian maturation. In addition, their expression levels were also significantly

Table 2
The top five most significantly enriched GO terms.

Compared groups	Biological process				Molecular function				Cellular component			
	GO terms	*q*-value	Up	Down	GO terms	*q*-value	Up	Down	GO terms	*q*-value	Up*	Down*
E0-E1	translation	0	123	592	structural molecule activity	0	209	538	ribosome	0	115	521
	protein metabolic process	1.34E-13	301	1420	structural constituent of ribosome	0	102	464	ribonucleoprotein complex	0	135	610
	proton transport	2.27E-05	12	95	structural constituent of cuticle	2.24E-14	96	8	cytosolic ribosome	1.04E-18	36	159
	hydrogen transport	2.89E-05	12	95	cysteine-type peptidase activity	3.50E-06	30	127	ribosomal subunit	1.20E-18	42	204
	cytoplasmic translation	2.22E-04	12	46	translation elongation factor activity	8.83E-06	19	70	extracellular region	1.29E-16	139	433
E1-E2	translation	0	592	116	structural molecule activity	0	601	183	periplasmic space	0	111	6
	small molecule metabolic process	2.39E-13	874	421	structural constituent of ribosome	0	466	88	cell envelope	0	98	6
	peptidoglycan metabolic process	1.82E-10	46	0	structural constituent of cuticle	1.77E-25	97	26	external encapsulating structure	0	154	21
	single-organism catabolic process	1.94E-10	473	213	phosphorelay response regulator activity	6.46E-10	31	0	external encapsulating structure part	0	90	6
	carboxylic acid metabolic process	5.46E-10	507	146	active transmembrane transporter activity	9.60E-10	227	97	cell outer membrane	0	68	4
E2-E3	translation	0	353	24	structural constituent of ribosome	0	262	15	ribosome	0	299	18
	protein metabolic process	5.80E-19	984	136	structural molecule activity	1.32E-26	324	79	ribonucleoprotein complex	9.94E-20	346	26
	sbmall molecule metabolic process	1.55E-05	569	108	structural constituent of cuticle	1.69E-25	40	48	cytosolic ribosome	4.51E-14	92	7
	proton transport	1.55E-05	64	2	structural molecule activity conferring elasticity	3.12E-06	18	5	extracellular region	5.30E-13	298	105
	hydrogen transport	2.18E-05	64	2	extracellular matrix constituent conferring elasticity	3.12E-06	18	5	cytosolic small ribosomal subunit	1.49E-11	51	3
E3-E4	small molecule metabolic process	6.09E-10	531	639	active transmembrane transporter activity	1.03E-08	136	159	cell periphery	0	834	469
	nucleoside phosphate metabolic process	6.09E-10	197	289	transmembrane transporter activity	2.01E-08	304	252	plasma membrane	0	800	441
	nucleotide metabolic process	6.09E-10	194	288	transporter activity	2.20E-08	361	301	periplasmic space	1.97E-25	5	109
	nucleobase-containing small molecule metabolic process	6.09E-10	211	305	phosphorelay response regulator activity	6.68E-08	0	34	cell envelope	3.80E-21	4	94
	organophosphate metabolic process	1.12E-09	266	330	purine nucleotide binding	2.33E-07	612	639	external encapsulating structure part	8.30E-18	3	86
E4-E0	translation	4.46E-09	183	234	structural molecule activity	0	169	370	extracellular region	3.66E-23	211	282
	protein metabolic process	1.52E-07	575	645	structural constituent of cuticle	0	6	138	ribosome	3.66E-17	157	225
					structural molecule activity conferring elasticity	1.37E-20	3	44	ribonucleoprotein complex	1.48E-08	199	252
					extracellular matrix constituent conferring elasticity	1.37E-20	3	44	cytosolic ribosome	5.88E-08	50	74
b					structural constituent of ribosome	2.57E-12	143	199	cytosolic part	1.31E-06	55	83

* The number of up-regulated and down-regulated DEGs enriched in each GO term in the former group of the compared groups.

Table 3
The top five most significantly enriched KEGG pathways.

Compared groups	KEGG Pathways	Up*	Down*
E0-E1	Ribosome	70	370
E1-E2	Ribosome	359	68
	Biosynthesis of amino acids	86	36
	Citrate cycle (TCA cycle)	68	8
E2-E3	Ribosome	200	12
	Other types of O-glycan biosynthesis	27	1
	Citrate cycle (TCA cycle)	36	4
E3-E4	Cell adhesion molecules (CAMs)	64	10
	MAPK signaling pathway	50	15
	Ribosome	27	215
	Focal adhesion	64	18
	Regulation of actin cytoskeleton	61	22
E4-E0	Ribosome	110	142

* The number of up-regulated and down-regulated DEGs enriched in each KEGG pathway in the former group of the compared groups.

decreased at the E4 stage when compared with the E0 stage (Fig. 5). Interestingly, we identified another 34 unigenes, the expression levels of which were the highest at the E0 stage with a sharp decline during ovarian maturation (Fig. 5; Table S6). The annotation results showed that these genes also encoded exoskeleton formation-related proteins, such as cuticle protein and chitin-binding protein. In addition, four unigenes (c99091_g1, c94442_g1, c112239_g1, c112325_g1) were annotated as the gastrolith protein (GAP). It was the first reported gastrolith-like protein in *L. vannamei*. The predicted protein (LvGAP) of unigene (c99091_g1) showed a sequence similarity of 70% with GAP 65 from *Cherax quadricarinatus*. Furthermore, bioinformatics analysis revealed that the LvGAP was also a member of the chitin-deacetylase family possessing the characteristic set of three domains: chitin-binding domain 2 (ChtBD2), low-density lipoprotein receptor class A domain (LDLa), and chitin-deacetylase domain (Fig. S8).

The unigene (c49610_g1) annotated as the farnesoic acid O-methyltransferase (FAMeT) was not differentially expressed during ovarian development. Nevertheless, the RPKM values suggested the possible higher expression levels of this gene with development of the ovary. qPCR analysis further detected an abundant expression of this gene in the eyestalk during all the stages of reproductive development and confirmed that the FAMeT had slightly higher expression levels in the eyestalks with ovary maturation, especially at the E4 stage (Fig. 3D).

qPCR analysis was performed on some of the unigenes mentioned above, including neuropeptides (Fig. 3A) and exoskeleton formation-related genes (Fig. 3B). The expression patterns of the selected genes determined by qPCR had good consistency with the RNA-seq results. In addition, we also selected several immune-related unigenes for qPCR validation, such as mannose-binding protein, prophenoloxidase activating enzyme 2, and serine proteinase inhibitor (Fig. 3C). These results could more comprehensively validate the reliability and accuracy of DEG analysis.

4. Discussion

As a crustacean species that dominates world shrimp production, *L. vannamei* is routinely brought into sexual maturation and ovulation in industry by the eyestalk ablation method. However, the procedure presumably also results in other hormonal imbalances and consequential detrimental effects, including high mortality. This study is the first report examining key genes and pathways involved in the ovarian maturation processes in the eyestalk by RNA-seq technology.

4.1. Functional enrichment analysis of GO terms and KEGG pathways

GO and KEGG enrichment analysis were able to assign biological processes related to various biological traits. Groups E0 and E4 were intact shrimp with different ovarian developmental stages, and comparison between the two groups identified the DEGs potentially involved in the natural maturation of ovary. Groups E1, E2, and E3 were eyestalk-ablated samples from different ovarian developmental stages, and comparisons of adjacent groups from the E0 group to the E3 group (E0-E1, E1-E2, and E2-E3) were intended to clarify the possible regulatory mechanism for the artificial induction of ovarian maturation. The biological process terms ‘translation’ and ‘protein metabolic process’, the molecular function terms ‘structural molecule activity’, ‘structural constituent of ribosome’, and ‘structural constituent of cuticle’, and the cellular component terms ‘ribosome’, ‘ribonucleoprotein complex’, ‘cytosolic ribosome’, and ‘extracellular region’ were all listed in the top five enriched GO terms; the KEGG pathway ‘ribosome’ was the most significantly enriched pathway when the adjacent groups from the E0 group to the E3 group are compared or the E0 group is compared to the E4 group. These results indicated that a large number of processes involved in protein synthesis were triggered to prepare for the regulation of ovarian development in the eyestalk. Moreover, similar enriched terms and pathways between the two comparisons suggested that the regulatory mechanism of ovarian development under natural

Table 4
The expression profiles of identified neuropeptides in the eyestalk during the ovarian maturation.

Gene ID	E0	E1	E2	E3	E4	NR Description
c108833_g1	5.17	16.19	1.54	4.70	1.80	hyperglycemic hormone-like peptide
c103865_g1	0	3.01	0.12	0.70	0	molt inhibiting hormone
c122023_g1	14.46	22.24	12.04	15.35	25.05	crustacean hyperglycemic hormone
c24357_g1	0.28	0.27	0	0	0	crustacean hyperglycemic hormone
c15356_g1	0	0.34	0.21	0	0.96	crustacean female sex hormone
c157867_g1	0	0.18	0.26	0	0.17	red pigment-concentrating hormone
c45163_g1	0.12	0.12	0	0	0.45	pigment-dispersing hormone 3
c83723_g1	0.12	1.47	0	0.22	0	pigment dispersing hormone II
c106238_g1	3.26	0.92	0.09	0.04	0.04	eclosion hormone
c107163_g1	214.56	247.17	291.69	167.59	251.20	neuroparsin
c98774_g1	105.42	90.42	229.90	208.92	139.51	neuroparsin
c113005_g1	19.39	13.09	25.09	38.59	33.81	neuroparsin
c109629_g1	1.40	0.66	0.70	1.23	0.18	bursicon beta subunit
c126398_g1	0.11	0	0	0.30	0.30	B-type preproallatostatin I
c80141_g1	0.19	0	0	0.06	0.80	crustacean cardioactive peptide
c28909_g1	0.25	0	0.39	0	0.08	preprotachykinin
c10160_g1	0.18	0	0.25	0	0.54	preprotachykinin
c95914_g1	0.51	0.72	0.39	0.69	0.30	Myomodulin neuropeptides 1
c98533_g1	368.16	351.07	222.15	939.85	243.10	FMRFamide-related peptides type HF-4

The gene ID, expression profile (RPKM value), and NR description is depicted.

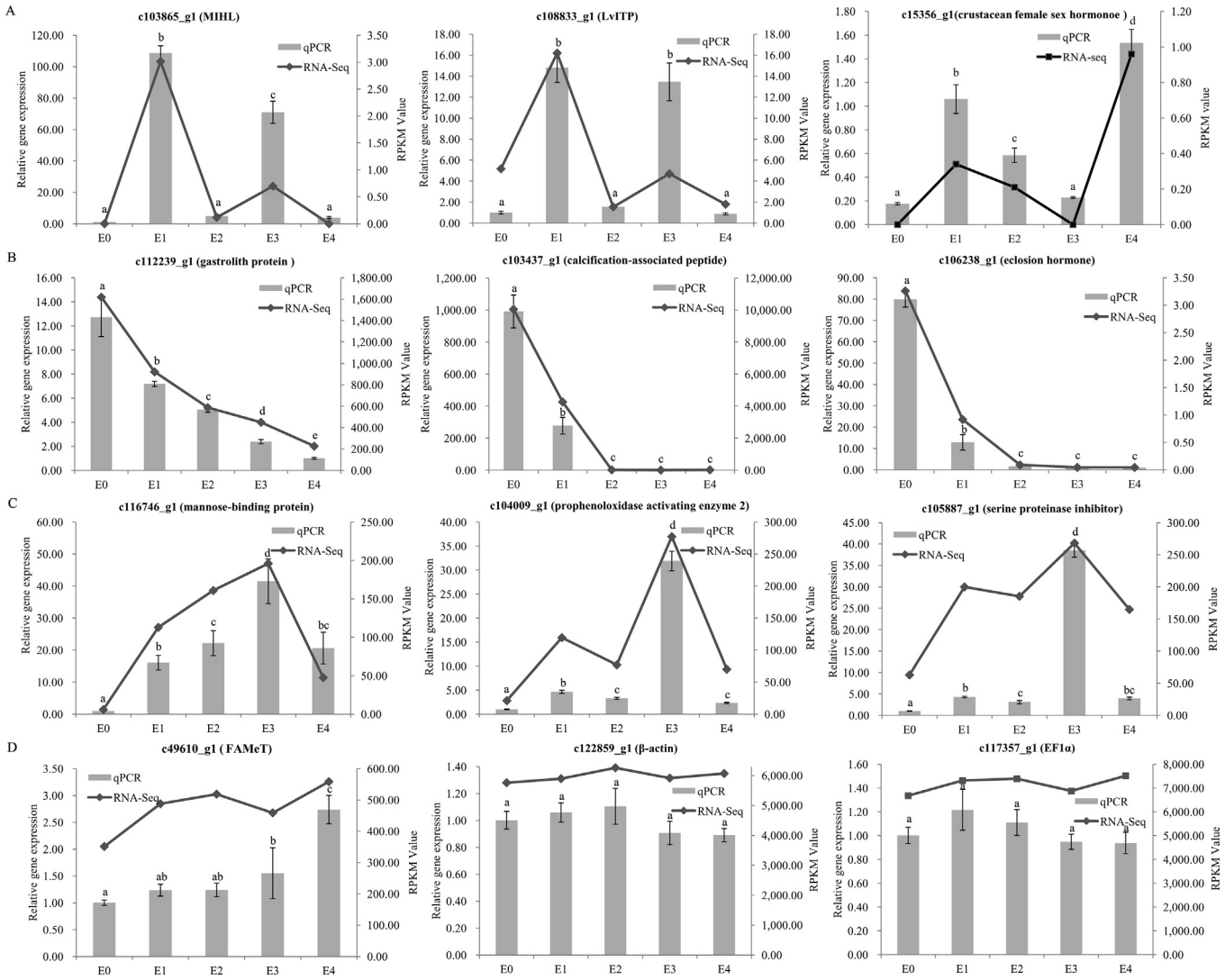

Fig. 3. Real-time quantitative PCR validation of RNA-seq data. Twelve unigenes were selected for validation, including neuropeptides (A), exoskeleton formation-related genes (B), immune-related genes (C), and non-differentially expressed genes (D), such as FAMeT and housekeeping genes. X axis represents the developmental stages. Columns and bars represent the means and standard error of relative expression levels from qPCR results (Y axis at left). Lines represent the FPKM value from transcriptome results (Y axis at right). Values with different superscripts indicated statistical significance ($p < 0.05$), which were calculated via one-way ANOVA.

conditions shared some characteristics with oogenesis induced by eyestalk ablation. The identified 59 exoskeleton formation-related unigenes were significantly down-regulated from the E0 to the E3 group and the E4 group (Fig. 5), which corresponded with the enriched molecular function term 'structural constituent of cuticle'. This suggests a potential negative regulation of exoskeleton formation-related genes during ovarian development.

The comparison between the E3 and the E4 groups showed different results in the enrichment analysis. The top five enriched biological process terms were all involved with 'metabolic process' instead of 'translation'. For molecular function terms, the top three enriched terms were related to the term 'transporter activity', while other comparisons were enriched for 'structural molecule activity'. In addition, most enriched cellular component terms specified cell membrane-related components, while it was the term 'ribosome' in other compared groups. As the ovaries of both groups were all at the S3-4 stage, these results imply differences in regulatory mechanisms between natural and artificial induced ovarian development.

4.2. Neuroendocrine regulation of the eyestalk during ovarian development

As the eyestalk is a major site for the production of neurohormones and regulates many physiological activities, including molting, growth, feeding, and reproduction (Christie et al., 2010b; Hopkins, 2012; Manfrin et al., 2015), we first focused our attention on transcripts belonging to endocrine pathways.

Proteins associated with term identifiers designating 'intracellular' or 'cellular membrane associated with receptors' were considered potential candidates for understanding the main activities of the eyestalk. G-protein coupled receptors (GPCRs) constitute a superfamily of seven transmembrane spanning proteins that respond to a diverse array of sensory and chemical stimuli, such as light, odor, taste, pheromones, hormones, and neurotransmitters (Ferguson, 2001). In this study, the identified fourteen GPCRs showed higher expression levels in E1, E2, or E3 groups after unilateral eyestalk ablation (Fig. 4). Seven unigenes showed highest levels early in the E1 stage. The homolog of two unigenes (c119632_g1, c115985_g1) is the lipoprotein receptor (*CasLpR*) from *C. sapidus,* which is involved in the defense system or the stress response of *C. sapidus* (Tsutsui and Chung, 2012). Therefore, the high expression of these unigenes in the E1 stage might respond to the stress

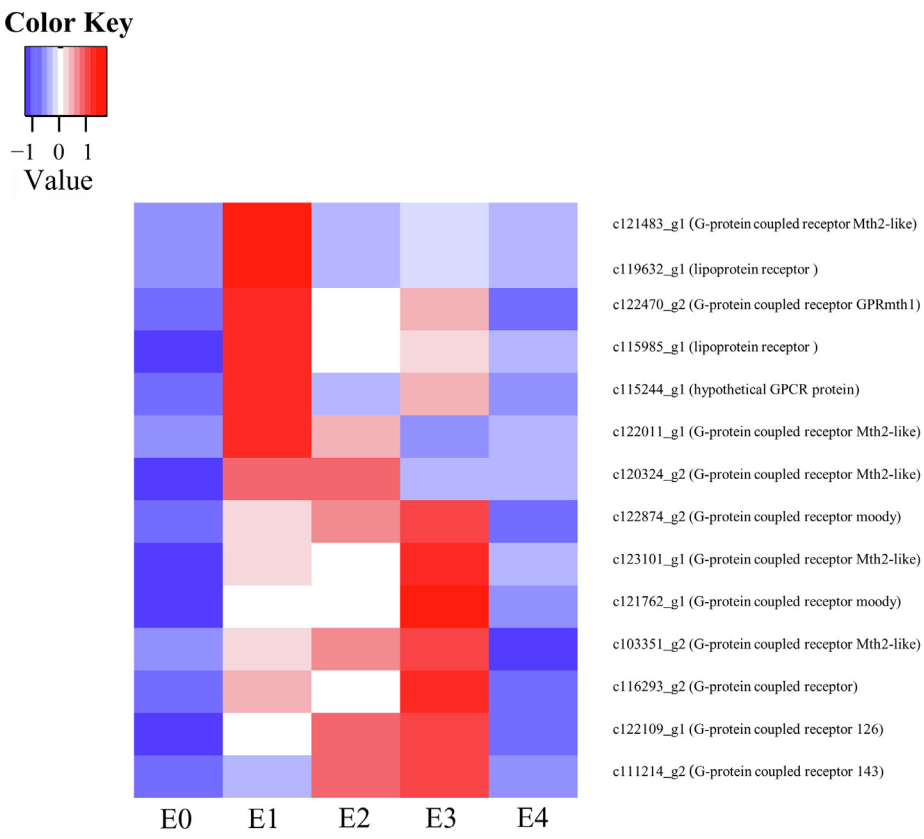

Fig. 4. Expression profiles of GPCRs in the eyestalk during ovary maturation. Heatmap colors represent relative mRNA expression as indicated in the Color key. The red color shows high expression, and the blue color represents lower levels of expression. The color from red to blue represents the log10 (RPKM + 1) from large to small.

and damage resulting from eyestalk ablation. The other seven GPCR-assigned unigenes showed an opposite pattern with highest levels late in the E3 stage. It is possible that the expressions of these receptors increased in response to the loss of basal hormone signals or the release of eyestalk neuropeptides caused by eyestalk ablation. In addition, the shrimp were artificially induced to mature in one week after the eyestalk ablation. It was possible that the higher expression of these GPCRs was involved in regulating the rapid maturation of ovary. Further functional characterization of the various hormone receptors in the eyestalk, including their modes of regulation and probable coupling to excitation-release mechanisms in the neurosecretory cells of the eyestalk, may offer additional opportunities for manipulation of eyestalk neuropeptide levels.

In this study, the expression of two CHH unigenes (c108833_g1, c103865_g1) was induced by eyestalk ablation with the highest level in the E1 stage when the ovary began to develop in the cephalothorax region. Their expression levels sharply declined at the E2 stage and increased again at the E3 stage (Fig. 3). The expression patterns of these genes showed some similarities with the GPCRs described above, suggesting a possible synergy between the two kinds of genes in reproductive regulation. In addition, the homologs of c108833_g1 (LvITP or CHH-B1) and c103865_g1 (MIHL) have been reported to be involved in hyperglycemic regulation, osmoregulation, and immune response. The LvITP transcript has been observed in the eyestalk, extra-eyestalk neuronal tissues such as the thoracic ganglion, brain, and ventral nerve, and in non-neuronal tissues such as the gut and gill, suggesting a potential role in osmoregulation (Tiu et al., 2007). Functional analysis confirmed the hyperglycemic and osmotic effects of recombinant CHH-B1 protein (Camacho-Jiménez et al., 2015; Camacho-Jiménez et al., 2017; Lago-Lestón et al., 2007). Recently, the MIHL protein was revealed to play important roles in antiviral and antibacterial immune responses in shrimp (Zuo et al., 2018). It has been suggested that all members of the CHH superfamily originated from a common ancestral gene through single-gene or genome duplication, and they may develop multiple biological functions as a consequence of gene duplication and divergence in crustaceans (Chan et al., 2003; Montagné et al., 2010). Therefore, further study is needed to explore their roles in other physiological processes related to reproduction in order to understand completely CHH peptide family relevance during the reproductive cycle of *L. vannamei*.

The CFSH was first purified from the female eyestalk of the blue crab *C. sapidus*, suggesting an essential role in the development of female secondary sexual characteristics (Zmora and Chung, 2014). In the kuruma prawn, *Marsupenaeus japonicus*, two CFSH isoforms were identified to be derived from distinct tissues, the eyestalk (Maj-CFSH-es) and ovary (Maj-CFSH-ov), and studies revealed that they may play a role in the orchestration of reproductive processes (Kotaka and Ohira, 2018; Tsutsui et al., 2018). In this study, the unigene (c15356_g1) annotated as the CFSH was significantly increased at the E4 stage, suggesting that it was involved in regulating vitellogenesis in shrimp with intact eyestalks. As there was no expression of the unigene (c15356_g1) in ovary during ovarian maturation in this study, we speculated that this putative Liv-CFSH may be specifically expressed in the eyestalk. For a comprehensive study of the CFSH function, the expression of this neuropeptide will have to be analyzed in the juvenile and subadult shrimp. Based on these results, further functional characterization of CFSH will be addressed using RNA-interference mediated gene knockdown and administration of recombinant hormone.

Eyestalk ablation has been extensively practiced in commercial shrimp culture as a technique to accelerate maturation of female gonads in crustaceans, which is based on the assumption that eyestalk removal diminishes VIH production (Hopkins, 2012; Okumura, 2007). However, in this study, the transcript of LvVIH was not detected in the eyestalks from either intact shrimp or unilateral eyestalk-ablated shrimp at any ovarian maturation stage. Furthermore, sequence alignment showed that the unigene (c24357_g1) had a high similarity with the neuropeptide SGP-G of *L. vannamei*, which has been reported to exhibit vitellogenesis inhibiting activity (Tsutsui et al., 2007; Tsutsui et al., 2013)

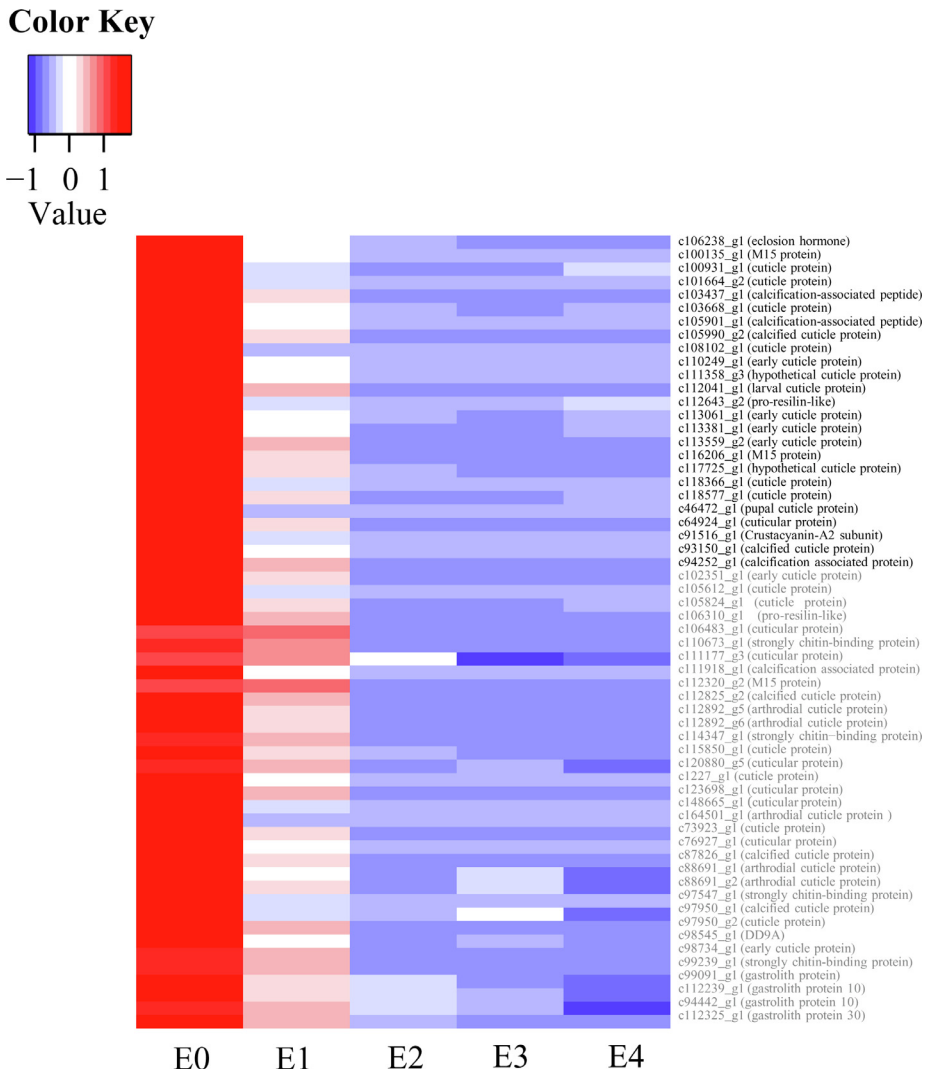

Fig. 5. Expression profiles of exoskeleton-formation related genes in the eyestalk during ovary maturation. Heatmap colors represent relative mRNA expression as indicated in the Color key. The red color shows high expression, and the blue color represents lower levels of expression. The color from red to blue represents the log10 (RPKM + 1) from large to small. The names with black fonts were down-regulated genes from E0 to E3 stage, and those with grey fonts were other down-regulated exoskeleton formation-related genes.

(Fig. S4C). Transcript levels of c24357_g1, however, were extremely low. The low relative expression levels of these transcripts suggested that GIH in the eyestalk may not be the main reason for hindering the maturation of the ovary. Perhaps the peptides in other organs may be responsible for the inhibitory effect. A previous study revealed that very high levels of LvVIH mRNA expression are observed in the brain in *L. vannamei*, surpassing even eyestalk LvVIH mRNA levels in relative terms, and eyestalk ablation could induce ovary maturation by not only removing the LvVIH production from the ablated eyestalk but also reducing the production of LvVIH from the brain (Chen et al., 2014). On the other hand, it is possible that other peptides in the eyestalk might have greater impacts on the regulation of ovarian development in parent shrimp. In this study, it is possible that eyestalk ablation induced ovary maturation by increasing the expression levels of the above two CHH peptides (c108833_g1, c103865_g1). This study suggests that crustacean reproduction is meditated by more CHH superfamily peptides than are currently known, and ablation of the eyestalk may influence crustacean reproduction by changing the circulating concentration of as yet unidentified CHH superfamily peptides.

4.3. Analysis of methyl farnesoate (MF) synthesis in the eyestalk in L. Vannamei

In crustaceans, MF participates in various physiological processes (Miyakawa et al., 2014), including molting (Taketomi et al., 1989; Tamone and Chang, 1993), reproduction (Olmstead and Leblanc, 2002; Reddy et al., 2004), morphogenesis (Laufer et al., 2005; Rotllant et al., 2000), and osmoregulation (Lovett et al., 1997; Lovett et al., 2006). FAMeT is the key enzyme responsible for the conversion of farnesoic acid (FA) to MF in the final step of MF synthesis using the cofactor S-adenosyl-L-methionine (Nagaraju, 2007). Although both FA and MF had been implicated as the major products of the mandibular organ (MO) (Laufer et al., 1987; Tobe et al., 1989), the constitutive expression of FAMeT in shrimp demonstrated that only small amounts of FA were converted to MF in the MO, and most of the FA was secreted to the hemolymph and converted to MF by FAMeT in the target tissues (Gunawardene et al., 2002; Hui et al., 2008). In this study, the unigene (c49610_g1) annotated as FAMeT showed considerable expression in the eyestalk, suggesting that the eyestalk was also a target tissue for the synthesis of MF. qPCR analysis further confirmed that the gene was expressed slightly higher in the eyestalks during the ovary maturation (Fig. 3D). Exogenous MF administration has been reported to result in

gonad stimulation in *Macrobrachium malcolmsonii* (Nagaraju et al., 2003), *Oziotelphusa senex senex* (Reddy et al., 2004), and *L. vannamei* (Alnawafleh et al., 2014). Thus, FAMeT may be involved in the regulation of the reproductive process in *L. vannamei* through the synthesis of MF. Further research is needed to detect the levels of FAMeT and MF in other tissues in order to establish the exact roles of FAMeT and MF in the control of reproduction in crustaceans.

4.4. Exoskeleton formation-related genes putatively involved in L. Vannamei reproduction

In insects, eclosion hormone, regulated by 20-hydroxyecdysone (20E) (Morton and Truman, 1988; Truman et al., 1983), evokes an ecdysis motor program (Clark et al., 2004) and triggers the shedding of the old cuticle at the end of each ecdysis (Ewer et al., 1994). In crustaceans, several eclosion hormone genes have been identified from *C. sapidus* (Christie et al., 2010a), *Euphausia crystallorophias* (Toullec et al., 2013), *Scylla paramamosain* (Bao et al., 2015), and *Exopalaemon carinicauda* (Zhou et al., 2017). Phylogenetic analysis confirmed that the unigene (c106238_g1) encoded the *L. vannamei* eclosion hormone (LvEH). In this study, we identified the down-regulation of LvEH and other exoskeleton formation-related genes during ovarian maturation. A functional study of EH in *E. carinicauda* revealed that EH probably played important roles in the molting process, although it showed different tissue expression profiles from that in insects (Zhou et al., 2017). As exoskeleton formation is closely related to the molting process in crustaceans, in-depth studies are needed to detect the expression patterns of LvEH during the molting cycle in *L. vannamei*.

It is well known that to generate a new exoskeleton, crayfish rely on gastroliths, which are cuticle-like structures that serve as temporary calcium storage organs and assist in the fast hardening of the new post-molt cuticle (Luquet and Marin, 2004; Travis, 1960; Ueno, 1980). The protein GAP 65 isolated from the gastrolith of *C. quadricarinatus* was demonstrated to play central roles in the formation of gastrolith and extracellular matrix and the functioning of mineral deposition during the biomineralization process (Glazer et al., 2015; Shechter et al., 2008). In this study, we also identified and characterized a unigene (c99091_g1) encoding a GAP 65 homolog with the characteristic set of three domains: chitin-binding domain 2 (ChtBD2), low-density lipoprotein receptor class A domain (LDLa), and chitin-deacetylase domain (Fig. S8). Of these, the LDLa domain has predicted calcium-binding ability (Rodenburg and Van der Horst, 2005). Unlike the crayfish, no gastrolith-like structure has been reported in shrimp. A previous study reported that calcium was mainly absorbed from the external environment, used to mineralize the cuticle of *L. vannamei*, and stored in the hemolymph and hepatopancreas (Greenaway, 1985; Li and Cheng, 2012). Therefore, on the one hand, the identification of LvGAP suggested that there may be new pathways for re-absorption and storage of calcium in *L. vannamei*, which needs further confirmation. On the other hand, in our dataset, 59 exoskeleton formation-related proteins showed similar expression patterns with the identified gastrolith proteins, including the EH, cuticle-like proteins, calcification-associated proteins, and chitin-binding proteins (Fig. 5). The cuticle protein is an important part of the exoskeleton. The crustacean cuticle provides initial reinforcement by cross-linking cuticle proteins attached to the cuticle chitin-fiber matrix. Considering the chitin-binding and calcium-binding abilities attributed to the ChtBD2 and LDLa domains of LvGAP (Rodenburg and Van der Horst, 2005; Tetreau et al., 2015), we speculate that LvGAP might function in the exoskeleton formation process, contributing to the calcification of cuticle proteins and the hardness of the exoskeleton.

In earlier studies, the exoskeleton formation-related genes were differentially expressed among different molting phases. For example, the transcripts encoding various cuticle proteins displayed molt-cycle stage specific differential expression in *Portunus pelagicus* (Kuballa et al., 2007). In *L. vannamei*, genes involved in exoskeleton formation, development, and construction, showed a strong coordination with a high degree of order during the molt cycle (Gao et al., 2017). However, in this study, these exoskeleton formation-related transcripts had the highest expression levels in the E0 stage when the ovary was undeveloped, while they showed poor expression levels in the E3 and the E4 stages when the ovary was mature. As the shrimp were all sampled in the inter-molt stage with different ovarian stages, it seemed that the expression of these exoskeleton formation-related transcripts could also be modulated by ovarian maturation stage besides the molting cycle. A similar phenomenon was also found in other crustacean species. The cuticle protein DD9B, determined to be up-regulated in epithelial cells in post-molt *M. japonicus* (Watanabe et al., 2000), was also up-regulated at pre-vitellogenic stage compared with the vitellogenic stage in the eyestalk of wild-caught *Penaeus monodon* during ovarian maturation (Brady et al., 2012). Furthermore, the down-regulation of these exoskeleton formation-related genes in this study suggested an antagonistic effect to reproduction. Several studies, describing the down-regulation and synchronization of vitellogenesis with the molt cycle, revealed molting as an antagonistic process to the reproductive cycle (Raviv et al., 2008). In *L. vannamei*, vitellogenin gene expression was high in the inter-molt/early pre-molt stages and was down-regulated immediately before and after ecdysis. The observed ovarian re-sorption in females between 1 and 3 days before ecdysis and the re-development of the ovaries approximately 1 day after ecdysis were in keeping with the quantities of *Vg* mRNA measured at these periods (Raviv et al., 2006). Chan (1995) reported that ovary maturation in Penaeidae occurred when the process of molting was in progress. Thus, the Penaeidae, like other crustaceans, have to manage the large energy requirement of both molting and reproduction, as vitellogenesis, the central event of the female reproductive cycle, and secretion of a new cuticle during molting could affect organism physiology through their competitive utilization of reserve materials from storage organs (Hartnoll, 2006; Nelson, 1991). Therefore, in this study, the down-regulated exoskeleton formation-related genes might be attributed to the competition between exoskeleton formation and reproduction for energy allocation. The measurement of circulating ecdysteroid concentration during ovarian development is needed to further clarify the relationship between this phenomenon and the molting process.

Hormonal interactions play a significant role in the regulation of nutritive supply for molting and reproduction processes. The crustacean MIH produced in the XO/SG negatively regulates molting by decreasing the circulating molt-stimulating hormone ecdysteroid that is synthesized in the Y-organ (Chang and Mykles, 2011). Previous studies have suggested that MIH may serve as one of the candidates for mediating the physiological process of molting and reproduction. In *Metapenaeus ensis*, *C. sapidus*, and *L. vannamei*, the action of MIH on molting and reproduction in females was antagonistic: MIH inhibited molting and stimulated vitellogenesis (Luo et al., 2015; Tiu and Chan, 2007; Zmora et al., 2009). As described in the former section, two CHH genes were differentially expressed during ovarian maturation. The expression of MIHL and ITP was induced by eyestalk ablation with the highest level in the E1 stage when the ovary began to develop in the cephalothorax region. Then, their expression levels sharply declined at the E2 stage and increased again at the E3 stage. It is possible that the MIHL and ITP genes might have a similar function to MIH in *L. vannamei* due to the duplication of the CHH superfamily in crustaceans (Chan et al., 2003; Montagné et al., 2010). Thus, the high expression of these CHH superfamily members hypothetically functioned to inhibit the expression of molting-related genes, including exoskeleton formation-related genes and promote the expression of *Vg* and probably other vitellogenesis-related genes. In fact, eyestalk ablation could induce the maturation of ovary several times during the reproductive cycle, along with shortening the molting cycle in *L. vannamei* (Arcos et al., 2005; Sainz-Hernández et al., 2008). As we only collected samples from shrimp during the first cycle of ovarian maturation, an in-depth study monitoring CHH gene expression relative to changes both in hemolymph

ecdysteroid titer and vitellogenin synthesis is needed to comprehensively examine the role of these peptides on molt progression and ovarian maturation.

5. Conclusions

This paper presents the first eyestalk transcriptome analysis to cover the complete and dynamic ovary maturation cycle in shrimp. The enrichment analysis of GO terms and KEGG pathways reveals similarities and differences between natural and artificially induced ovarian maturation. It also establishes a transcriptional scenario for the regulation of ovarian development and examines the transcriptional events involved from several perspectives, including neuroendocrine regulation in the eyestalk, and the down-regulation of exoskeleton formation-related genes during ovarian development. Moreover, it provides novel insights into the molecular processes underlying these transcriptional events. It indicates that a complex regulatory network is involved in the regulation of ovary development in *L. vannamei*. These results enhance our understanding of reproductive regulation in shrimp and provide an experimental blueprint for future research on eyestalk regulation for growth and reproduction in other crustaceans.

Acknowledgments

This work was supported by the Central Public-interest Scientific Institution Basal Research Fund CAFS, China (2016HY-ZD04; 2018GH12; 20603022016006), China Postdoctoral Science Foundation, China (2016M592272), Shandong Province Postdoctoral Innovative Foundation, China (201602008), Qingdao Postdoctoral Application Research Foundation, China (No.2016235), Taishan Scholar Program For Seed Industry, China (Multi-Traits Selective Breeding of New Variety and ItsIndustrialization), China Agriculture Research System-48, China (CARS-48), Project of technical system of breeding aquatic variety supported by Guangdong province, China (zj002), and Key research and development project of Shandong Province, China (2016GSF115030). We also appreciate the help from Beijing ANNOROAD Bioinformatics Technology Co., Ltd in library construction and data processing.

Appendix A. Supplementary data

Supplementary data to this article can be found online at https://doi.org/10.1016/j.ygcen.2019.01.002.

References

Arcos, F.G., Palacios, E., Ibarra, A.M., Racotta, I.S., 2005. Larval quality in relation to consecutive spawnings in white shrimp *Litopenaeus vannamei* Boone. Aquac. Res. 36 (9), 890–897.
Alnawafleh, T., Kim, B.K., Kang, H.E., Yoon, T.H., Kim, H.W., 2014. Stimulation of molting and ovarian maturation by Methyl Farnesoate in the pacific white shrimp *Litopenaeus vannamei* (Boone, 1931). Fish Aquatic. Sci. 17, 115–121.
Bao, C., Yang, Y., Huang, H., Ye, H., 2015. Neuropeptides in the cerebral ganglia of the mud crab, *Scylla paramamosain*: transcriptomic analysis and expression profiles during vitellogenesis. Sci. Rep. 5, 17055.
Benzie, J.A., 1998. Penaeid genetics and biotechnology. Aquaculture 164, 23–47.
Brady, P., Elizur, A., Williams, R., Cummins, S.F., Knibb, W., 2012. Gene expression profiling of the cephalothorax and eyestalk in *Penaeus monodon* during ovarian maturation. Int. J. Biol. Sci. 8, 328.
Browdy, C., Samocha, T., 1985. The effect of eyestalk ablation on spawning, molting and mating of *Penaeus semisulcatus* de Haan. Aquaculture 49, 19–29.
Camacho-Jiménez, L., Díaz, F., Muñoz-Márquez, M.E., Farfán, C., Re, A.D., Ponce-Rivas, E., 2017. Hyperglycemic and osmotic effects of dopamine and recombinant hormone CHH-B1 in the Pacific white shrimp *Litopenaeus vannamei*. Mar. Freshwater Behav. Physiol. 50, 67–79.
Camacho-Jiménez, L., Sánchez-Castrejón, E., Ponce-Rivas, E., Munoz-Márquez, M.E., Aguilar, M.B., Re, A.D., Díaz, F., 2015. Hyperglycemic activity of the recombinant crustacean hyperglycemic hormone B1 isoform (CHH-B1) of the Pacific white shrimp *Litopenaeus vannamei*. Peptides 71, 32–39.
Chan, S.M., 1995. Possible roles of 20-hydroxyecdysone in the control of ovary maturation in the white shrimp *Penaeus vannamei* (Crustacea: Decapoda). Comp. Biochem. Physiol. C. 112, 51–59.
Chan, S.M., Gu, P.L., Chu, K.H., Tobe, S.S., 2003. Crustacean neuropeptide genes of the CHH/MIH/GIH family: implications from molecular studies. Gen. Comp. Endocrinol. 134, 214–219.
Chang, E.S., Mykles, D.L., 2011. Regulation of crustacean molting: a review and our perspectives. Gen. Comp. Endocrinol. 172, 323–330.
Chen, H.Y., Watson, R.D., Chen, J.C., Liu, H.F., Lee, C.Y., 2007. Molecular characterization and gene expression pattern of two putative molt-inhibiting hormones from *Litopenaeus vannamei*. Gen. Comp. Endocrinol. 151, 72–81.
Chen, T., Zhang, L.P., Wong, N.K., Zhong, M., Ren, C.H., Hu, C.Q., 2014. Pacific white shrimp (*Litopenaeus vannamei*) vitellogenesis-inhibiting hormone (VIH) is predominantly expressed in the brain and negatively regulates hepatopancreatic vitellogenin (VTG) gene expression. Biol. Reprod. 90, 47.
Christie, A.E., Durkin, C.S., Hartline, N., Ohno, P., Lenz, P.H., 2010a. Bioinformatic analyses of the publicly accessible crustacean expressed sequence tags (ESTs) reveal numerous novel neuropeptide-encoding precursor proteins, including ones from members of several little studied taxa. Gen. Comp. Endocrinol. 167, 164–178.
Christie, A.E., Stemmler, E.A., Dickinson, P.S., 2010b. Crustacean neuropeptides. Cell. Mol. Life Sci. 67, 4135–4169.
Clark, A.C., del Campo, M.L., Ewer, J., 2004. Neuroendocrine control of larval ecdysis behavior in *Drosophila*: complex regulation by partially redundant neuropeptides. J. Neurosci. 24, 4283–4292.
Corteel, M., Dantas-Lima, J.J., Wille, M., Alday-Sanz, V., Pensaert, M.B., Sorgeloos, P., Nauwynck, H.J., 2012. Moult cycle of laboratory-raised *Penaeus* (*Litopenaeus*) *vannamei* and *P. monodon*. Aquacult. Int. 20, 13–18.
Dai, P., Luan, S., Lu, X., Luo, K., Kong, J., 2017. Comparative transcriptome analysis of the Pacific White Shrimp (*Litopenaeus vannamei*) muscle reveals the molecular basis of residual feed intake. Sci. Rep. 7, 10483.
Ewer, J., De Vente, J., Truman, J.W., 1994. Neuropeptide induction of cyclic GMP increases in the insect CNS: resolution at the level of single identifiable neurons. J. Neurosci. 14, 7704–7712.
Ferguson, S.S., 2001. Evolving concepts in G protein-coupled receptor endocytosis: the role in receptor desensitization and signaling. Pharmacol. Rev. 53, 1–24.
Gao, Y., Wei, J., Yuan, J., Zhang, X., Li, F., Xiang, J., 2017. Transcriptome analysis on the exoskeleton formation in early developmetal stages and reconstruction scenario in growth-moulting in *Litopenaeus vannamei*. Sci. Rep. 7, 1098.
Glazer, L., Roth, Z., Weil, S., Aflalo, E.D., Khalaila, I., Sagi, A., 2015. Proteomic analysis of the crayfish gastrolith chitinous extracellular matrix reveals putative protein complexes and a central role for GAP 65. J. Proteomics 128, 333–343.
Grabherr, M.G., Haas, B.J., Yassour, M., Levin, J.Z., Thompson, D.A., Amit, I., Adiconis, X., Fan, L., Raychowdhury, R., Zeng, Q.D., Chen, Z.H., Mauceli, E., Hacohen, N., Gnirke, A., Rhind, N., di Palma, F., Birren, B.W., Nusbaum, C., Lindblad-Toh, K., Friedman, N., Regev, A., 2011. Full-length transcriptome assembly from RNA-Seq data without a reference genome. Nat. Biotechnol. 29, 644–652.
Greenaway, P., 1985. Calcium balance and moulting in the Crustacea. Biol. Rev. 60, 425–454.
Gunawardene, Y.I.N.S., Tobe, S.S., Bendena, W.G., Chow, B.K.C., Yagi, K.J., Chan, S.M., 2002. Function and cellular localization of farnesoic acid O-methyltransferase (FAMeT) in the shrimp, *Metapenaeus ensis*. Eur. J. Biochem. 269, 3587–3595.
Hartnoll, R., 2006. Reproductive investment in Brachyura. Hydrobiologia 557, 31–40.
Hopkins, P.M., 2012. The eyes have it: a brief history of crustacean neuroendocrinology. Gen. Comp. Endocrinol. 175, 357–366.
Hui, J.H.L., Tobe, S.S., Chan, S.M., 2008. Characterization of the putative farnesoic acid O-methyltransferase (LvFAMeT) cDNA from white shrimp, *Litopenaeus vannamei*: Evidence for its role in molting. Peptides 29, 252–260.
Jrdeo, C., Zhao, B., Malecha, S., Ako, H., Yang, J., 2006. Morphological and biochemical changes in the muscle of the marine shrimp *litopenaeus vannamei* during the molt cycle. Aquaculture 261, 688–694.
Kotaka, S., Ohira, T., 2018. cDNA cloning and in situ localization of a crustacean female sex hormone-like molecule in the kuruma prawn *Marsupenaeus japonicus*. Fish. Sci. 84, 53–60.
Kuballa, A.V., Merritt, D.J., Elizur, A., 2007. Gene expression profiling of cuticular proteins across the moult cycle of the crab *Portunus pelagicus*. BMC Biol. 5, 1–26.
Lago-Lestón, A., Ponce, E., Muñoz, M.E., 2007. Cloning and expression of hyperglycemic (CHH) and molt-inhibiting (MIH) hormones mRNAs from the eyestalk of shrimps of *Litopenaeus vannamei* grown in different temperature and salinity conditions. Aquaculture 270, 343–357.
Langmead, B., Salzberg, S.L., 2012. Fast gapped-read alignment with Bowtie 2. Nat. Methods 9, 357–359.
Laufer, H., Borst, D., Baker, F.C., Reuter, C.C., Tsai, L.W., Schooley, D.A., Carrasco, C., Sinkus, M., 1987. Identification of a juvenile hormone-like compound in a crustacean. Science 235, 202–205.
Laufer, H., Demir, N., Pan, X.J., Stuart, J.D., Ahl, J.S.B., 2005. Methyl farnesoate controls adult male morphogenesis in the crayfish *Procambarus clarkii*. J. Insect Physiol. 51, 379–384.
Li, C.H., Cheng, S.Y., 2012. Variation of calcium levels in the tissues and hemolymph of *Litopenaeus vannamei* at various molting stages and salinities. J. Crustacean Biol. 32, 101–108.
Livak, K.J., Schmittgen, T.D., 2001. Analysis of relative gene expression data using real-time quantitative PCR and the $2^{-\Delta\Delta CT}$ method. Methods 25, 402–408.
Lovett, D.L., Clifford, P.D., Borst, D.W., 1997. Physiological stress elevates hemolymph levels of methyl farnesoate in the green crab *Carcinus maenas*. Biol. Bull. 193, 266–267.
Lovett, D.L., Tanner, C.A., Glomski, K., Ricart, T.M., Borst, D.W., 2006. The effect of seawater composition and osmolality on hemolymph levels of methyl farnesoate in the green crab *Carcinus maenas*. Comp. Biochem. Physiol. A. 143, 67–77.

Lu, X., Kong, J., Luan, S., Dai, P., Meng, X., Cao, B., Luo, K., 2016. Transcriptome Analysis of the Hepatopancreas in the Pacific White Shrimp (*Litopenaeus vannamei*) under Acute Ammonia Stress. PLoS One 11 e0164396.
Luo, X., Chen, T., Zhong, M., Jiang, X., Zhang, L., Ren, C., Hu, C., 2015. Differential regulation of hepatopancreatic vitellogenin (VTG) gene expression by two putative molt-inhibiting hormones (MIH1/2) in Pacific white shrimp (*Litopenaeus vannamei*). Peptides 68, 58–63.
Luquet, G., Marin, F., 2004. Biomineralisations in crustaceans: storage strategies. C. R. Palevol 3, 515–534.
Manfrin, C., Tom, M., De Moro, G., Gerdol, M., Giulianini, P.G., Pallavicini, A., 2015. The eyestalk transcriptome of red swamp crayfish *Procambarus clarkii*. Gene 557, 28–34.
Martin, M., 2011. Cutadapt removes adapter sequences from high-throughput sequencing read. EMBnet J. 17, 10–12.
Miyakawa, H., Toyota, K., Sumiya, E., Iguchi, T., 2014. Comparison of JH signaling in insects and crustaceans. Curr. Opin. Insect Sci. 1, 81–87.
Montagné, N., Desdevises, Y., Soyez, D., Toullec, J.-Y., 2010. Molecular evolution of the crustacean hyperglycemic hormone family in ecdysozoans. BMC Evol. Biol. 10, 62.
Mortazavi, A., Williams, B.A., McCue, K., Schaeffer, L., Wold, B., 2008. Mapping and quantifying mammalian transcriptomes by RNA-Seq. Nat. Methods 5, 621–628.
Morton, D.B., Truman, J.W., 1988. The EGPs: the eclosion hormone and cyclic GMP-regulated phosphoproteins. II. Regulation of appearance by the steroid hormone 20-hydroxyecdysone in *Manduca sexta*. J. Neurosci. 8, 1338–1345.
Nagaraju, G.P.C., 2007. Is methyl farnesoate a crustacean hormone? Aquaculture 272, 39–54.
Nagaraju, G.P.C., Suraj, N., Reddy, P.S., 2003. Methyl farnesoate stimulates gonad development in *Macrobrachium malcolmsonii* (H. Milne Edwards)(Decapoda, Palaemonidae). Crustaceana 76, 1171–1178.
Nelson, K., 1991. Scheduling of reproduction in relation to molting and growth in malacostracan crustaceans. In: Kuris, A. (Ed.), Crustacean Egg Production. CRC Press, Boca Raton, pp. 77–116.
Okumura, T., 2007. Effects of bilateral and unilateral eyestalk ablation on vitellogenin synthesis in immature female kuruma prawns, *Marsupenaeus japonicus*. Zool. Sci. 24, 233–240.
Olmstead, A.W., Leblanc, G.A., 2002. Juvenoid hormone methyl farnesoate is a sex determinant in the crustacean *Daphnia magna*. J. Exp. Zool. A. 293, 736–739.
Palacios, E., Perez-Rostro, C.I., Ramirez, J.L., Ibarra, A.M., Racotta, I.S., 1999. Reproductive exhaustion in shrimp (*Penaeus vannamei*) reflected in larval biochemical composition, survival and growth. Aquaculture 171, 309–321.
Raviv, S., Parnes, S., Sagi, A., 2008. Coordination of reproduction and molt in decapods. In: Mente, E.E. (Ed.), Reproductive Biology of Crustaceans: Case Studies of Decapod Crustaceans. Science Publishers, Enfield, pp. 365–390.
Raviv, S., Parnes, S., Segall, C., Davis, C., Sagi, A., 2006. Complete sequence of *Litopenaeus vannamei* (Crustacea: Decapoda) vitellogenin cDNA and its expression in endocrinologically induced sub-adult females. Gen. Comp. Endocrinol. 145, 39–50.
Reddy, P.R., Nagaraju, G.P.C., Reddy, P.S., 2004. Involvement of methyl farnesoate in the regulation of molting and reproduction in the freshwater crab *Oziotelphusa senex senex*. J. Crustacean Biol. 24, 511–515.
Rodenburg, K.W., Van der Horst, D.J., 2005. Lipoprotein-mediated lipid transport in insects: analogy to the mammalian lipid carrier system and novel concepts for the functioning of LDL receptor family members. BBA-Mol. Cell. Biol. L. 1736, 10–29.
Rotllant, G., Takac, P., Liu, L., Scott, G.L., Laufer, H., 2000. Role of ecdysteroids and methyl farnesoate in morphogenesis and terminal moult in polymorphic males of the spider crab *Libinia emarginata*. Aquaculture 190, 103–118.
Saha, S., Sparks, A.B., Rago, C., Akmaev, V., Wang, C.J., Vogelstein, B., Kinzler, K.W., Velculescu, V.E., 2002. Using the transcriptome to annotate the genome. Nat. Biotechnol. 20 (5), 508.
Sainz-Hernández, J.C., Racotta, I.S., Dumas, S., Hernández-López, J., 2008. Effect of unilateral and bilateral eyestalk ablation in *Litopenaeus vannamei* male and female on several metabolic and immunologic variables. Aquaculture 283, 188–193.
Shechter, A., Glazer, L., Cheled, S., Mor, E., Weil, S., Berman, A., Bentov, S., Aflalo, E.D., Khalaila, I., Sagi, A., 2008. A gastrolith protein serving a dual role in the formation of an amorphous mineral containing extracellular matrix. Proc. Natl. Acad. Sci. U.S.A. 105, 7129–7134.
Taketomi, T., Motono, M., Miyawaki, M., 1989. On the biological function of the mandibular gland of decapod crustacea. Cell Biol. Int. Rep. 13, 463–469.
Tamone, S.L., Chang, E.S., 1993. Methyl farnesoate stimulates ecdysteroid secretion from crab Y-organs in vitro. Gen. Comp. Endocrinol. 89, 425–432.
Tan-Fermin, J.D., Pudadera, R.A., 1989. Ovarian maturation stages of the wild giant tiger prawn, *Penaeus monodon* Fabricius. Aquaculture 77, 229–242.
Tetreau, G., Dittmer, N.T., Cao, X., Agrawal, S., Chen, Y.R., Muthukrishnan, S., Haobo, J., Blissard, G.W., Kanost, M.R., Wang, P., 2015. Analysis of chitin-binding proteins from Manduca sexta provides new insights into evolution of peritrophin A-type chitin-binding domains in insects. Insect Biochem. Mol. Biol. 62, 127–141.
Tiu, S.H., He, J.G., Chan, S.M., 2007. The LvCHH-ITP gene of the shrimp (*Litopenaeus vannamei*) produces a widely expressed putative ion transport peptide (LvITP) for osmo-regulation. Gene 396, 226–235.
Tiu, S.H.K., Chan, S.M., 2007. The use of recombinant protein and RNA interference approaches to study the reproductive functions of a gonad-stimulating hormone from the shrimp *Metapenaeus ensis*. FEBS J. 274, 4385–4395.
Tobe, S., Young, D., Khoo, H., Baker, F., 1989. Farnesoic acid as a major product of release from crustacean mandibular organs in vitro. J. Exp. Zool. A. 249, 165–171.
Toullec, J.Y., Corre, E., Bernay, B., Thorne, M.A., Cascella, K., Ollivaux, C., Henry, J., Clark, M.S., 2013. Transcriptome and peptidome characterisation of the main neuropeptides and peptidic hormones of a euphausiid: the Ice Krill. *Euphausia crystallorophias*. PLoS One 8 e71609.
Travis, D.F., 1960. The deposition of skeletal structures in the crustacea. I. The histology of the gastrolith skeletal tissue complex and the gastrolith in the crayfish, *Orconectes (Cambarus) virilis* Hagen-Decapoda. Biol. Bull. 118, 137–149.
Truman, J.W., Rountree, D.B., Reiss, S.E., Schwartz, L.M., 1983. Ecdysteroids regulate the release and action of eclosion hormone in the tobacco hornworm, *Manduca sexta* (L.). J. Insect Physiol. 29, 895–900.
Tsutsui, N., Chung, J.S., 2012. A novel putative lipoprotein receptor (CasLpR) in the hemocytes of the blue crab, *Callinectes sapidus*: cloning and up-regulated expression after the injection of LPS and LTA. Fish Shellfish Immunol. 32, 469–475.
Tsutsui, N., Kotaka, S., Ohira, T., Sakamoto, T., 2018. Characterization of distinct ovarian isoform of crustacean female sex hormone in the kuruma prawn *Marsupenaeus japonicus*. Comp. Biochem. Physiol. A. 217, 7–16.
Tsutsui, N., Ohira, T., Kawazoe, I., Takahashi, A., Wilder, M.N., 2007. Purification of sinus gland peptides having vitellogenesis-inhibiting activity from the whiteleg shrimp *Litopenaeus vannamei*. Mar. Biotechnol. 9, 360.
Tsutsui, N., Ohira, T., Okutsu, T., Shinji, J., Bae, S.-H., Kang, B.J., Wilder, M.N., 2013. Molecular cloning of a cDNA encoding vitellogenesis-inhibiting hormone in the whiteleg shrimp *Litopenaeus vannamei* and preparation of its recombinant peptide using an *E. coli* expression system. Fish. Sci. 79, 357–365.
Ueno, M., 1980. Calcium transport in crayfish gastrolith disc: morphology of gastrolith disc and ultrahistochemical demonstration of calcium. J. Exp. Zool. A Ecol. Integr. Physiol. 213, 161–171.
Vandesompele, J., De Preter, K., Pattyn, F., Poppe, B., Van Roy, N., De Paepe, A., Speleman, F., 2002. Accurate normalization of real-time quantitative RT-PCR data by geometric averaging of multiple internal control genes. Genome Biol. 3 research0034-1.
Wang, L.K., Feng, Z.X., Wang, X., Wang, X.W., Zhang, X.G., 2010. DEGseq: an R package for identifying differentially expressed genes from RNA-seq data. Bioinformatics 26, 136–138.
Watanabe, T., Persson, P., Endo, H., Kono, M., 2000. Molecular analysis of two genes, DD9A and B, which are expressed during the postmolt stage in the decapod crustacean *Penaeus japonicus*. Comp. Biochem. Physiol. B. 125, 127–136.
Webster, S.G., Keller, R., Dircksen, H., 2012. The CHH-superfamily of multifunctional peptide hormones controlling crustacean metabolism, osmoregulation, moulting, and reproduction. Gen. Comp. Endocrinol. 175, 217–233.
Wei, J., Zhang, X., Yu, Y., Huang, H., Li, F., Xiang, J., 2014. Comparative transcriptomic characterization of the early development in Pacific white shrimp *Litopenaeus vannamei*. PLoS One 9 e106201.
Wu, J., Mao, X., Cai, T., Luo, J., Wei, L., 2006. KOBAS server: a web-based platform for automated annotation and pathway identification. Nucleic Acids Res. 34, W720–W724.
Zhao, S., Fernald, R.D., 2005. Comprehensive algorithm for quantitative real-time polymerase chain reaction. J. Comput. Biol. 12, 1047–1064.
Zhou, L., Li, S., Wang, Z., Li, F., Xiang, J., 2017. An eclosion hormone-like gene participates in the molting process of Palaemonid shrimp *Exopalaemon carinicauda*. Dev. Genes Evol. 227, 189–199.
Zmora, N., Chung, J.S., 2014. A novel hormone is required for the development of reproductive phenotypes in adult female crabs. Endocrinology 155, 230–239.
Zmora, N., Trant, J., Zohar, Y., Chung, J.S., 2009. Molt-inhibiting hormone stimulates vitellogenesis at advanced ovarian developmental stages in the female blue crab, *Callinectes sapidus* 1: an ovarian stage dependent involvement. Saline Syst. 5, 7.
Zuo, H., Yuan, J., Niu, S., Yang, L., Weng, S., He, J., Xu, X., 2018. A molting-inhibiting hormone-like protein from Pacific white shrimp *Litopenaeus vannamei* is involved in immune responses. Fish Shellfish Immunol. 72, 544–551.